IEEE Access
Multidisciplinary | Rapid Review | Open Access Journal

Received August 30, 2019, accepted October 21, 2019, date of publication November 4, 2019, date of current version November 14, 2019.

Digital Object Identifier 10.1109/ACCESS.2019.2951376

Brain Rhythm Sequencing Using EEG Signals: A Case Study on Seizure Detection

JIA WEN LI[1,2,3], (Student Member, IEEE), SHOVAN BARMA[4], (Member, IEEE), PENG UN MAK[1], (Senior Member, IEEE), SIO HANG PUN[2,3], (Senior Member, IEEE), AND MANG I VAI[1,2,3], (Senior Member, IEEE)

[1]Department of Electrical and Computer Engineering, University of Macau, Macau 999078, China
[2]State Key Laboratory of Analog and Mixed-Signal VLSI, University of Macau, Macau 999078, China
[3]Institute of Microelectronics, University of Macau, Macau 999078, China
[4]Department of Electronics and Communication Engineering, Indian Institute of Information Technology Guwahati (IIITG), Guwahati 781015, India

Corresponding author: Peng Un Mak (fstpum@umac.mo)

This work was funded in part by The Science and Technology Development Fund (FDCT), Macau SAR (file no. 093/2015/A3 and 088/2016/A2), and in part by the Research Committee of the University of Macau under Grant MYRG2015-00178-AMSV, Grant MYRG2016-00157-AMSV, Grant MYRG2018-00146-AMSV, and Grant MYRG2019-00056-AMSV.

ABSTRACT A technique based on five brain rhythms (δ, θ, α, β, and γ) presented in the sequence for analyzing Electroencephalography (EEG) signals has been proposed. First, the production of the sequence has been accomplished by selecting the prominent brain rhythm having the maximum instantaneous power at specific timestamp consecutively throughout the EEG. To this purpose, the reassigned smoothed pseudo Wigner-Ville distribution (RSPWVD) has been employed. Then, in order to verify the proposed technique and evaluate its performance, a case study of seizure detection has been implemented. As experimental validation, 93 patients from the Karunya database have been investigated. Moreover, to characterize the brain rhythm sequence for seizure detection, two additional indices derived from the power discharge and synchronous behavior have been applied. Results show that the particular rhythm pattern during the seizure is usually one type (either δ, θ, or α) and it is subject-dependent. Hence, by focusing on the changes of such particular rhythm through the two indices, the time-related occurrences of seizures can be determined in detail. Meanwhile, the representative channels for seizure detection can be found by studying the similarity of sequences, which are helpful to reduce the number of applied channels. Finally, the proposed technique provides an accuracy of 98.9%, which demonstrates it is competent to detect the appearances of abnormal seizures from the EEG signals reliably. Consequently, the brain rhythm sequencing could open a new way to interpret and characterize the EEG in various applications such as for epileptic patients.

INDEX TERMS Brain rhythm sequencing, electroencephalography (EEG), time-frequency analysis (TFA), reassigned smoothed pseudo Wigner-Ville distribution (RSPWVD), seizure detection.

I. INTRODUCTION

As a tool that is commonly used for assessing the electrical activities of the brain, electroencephalography (EEG) is valuable. It is an electrophysiological monitoring technique that records the time-varying potential variations produced by the firings of neurons and has a high time resolution that captures changes within the millisecond timeframe. Further, since EEG presents non-linear, non-stationary, and dynamic property [1]. Therefore, in order to distinguish the traces of EEG in different brain activities, the proper analysis and characterization of the EEG signals are essential. So far, a number of approaches have been applied for EEG signals analysis, such as linear prediction (LP) [2] and independent component analysis (ICA) [3] in time domain; the spectral analysis [4], [5] in frequency domain; Short-time Fourier transform (STFT) [6], Hilbert-Huang transform (HHT) [7], Wigner-Ville distribution (WVD) [8], [9], and wavelet transform (WT) [10]–[12] in time-frequency domain; and special types like singular value decomposition (SVD) [13], recurrence quantification analysis (RQA) [14], and so on.

Regarding the time domain analysis, the changes of EEG signals over time have been recorded so that a good temporal resolution can be acquired. Further, as the EEG signals in the

The associate editor coordinating the review of this manuscript and approving it for publication was Alberto Botter.

time domain are mostly amplitude related, so the electrical discharges at different timestamps can be easily visualized. Nonetheless, the spectral information of EEG is ignored. In contrast, in the spectral analysis of the frequency domain, the time-related information such as the corresponding duration of events or the time transformations between different brain activities is missing. As a result, compared with the time or the frequency analysis, the time-frequency analysis (TFA) by applying STFT, HHT, WVD, WT, etc. is preferred. As for TFA, each method owns its advantages and disadvantages to deal with the EEG signals. For instance, in STFT, the whole EEG signals are divided into small segments and a window function whose width is equal to the segment of the signals is employed [6]. Nevertheless, the main drawback of STFT is the finite length window that the narrow window provides better time resolution and poor frequency resolution, while the broad window produces better frequency resolution and poor time resolution. So, in order to overcome the resolution issue, WT has been proposed as a solution; WT has a facility of varying frequency components such as the narrow window size for high frequency and the broad one for low frequency. In WT, a mother wavelet is used and it is shifted continually along the time scale for calculating the wavelet coefficients. By applying WT, the EEG signals can be decomposed into certain sub-bands with good resolution. However, it is limited by its poor directionality, shift sensitivity, and lack of phase information [15]; About WVD, it has several desirable properties for analyzing the non-linear and non-stationary EEG signals, such as tracking the sudden changes of the signals in the time domain and preserving both the time and frequency shift information. But, unnecessary cross-terms will appear [16]; In HHT, it is a technique derived from the empirical basic functions and EEG signals are decomposed into a set of the intrinsic mode functions (IMFs) through the empirical mode decomposition (EMD) process. Hence, HHT is beneficial to calculate the instantaneous frequencies and amplitudes of the EEG signals. Nonetheless, due to the end effect of EMD resulting on both ends of the data set meaningless, the capability of HHT for dealing with power quality analysis could be influenced [17]. Then, concerning SVD, it is a decomposition approach for reducing a matrix to its constituent parts in order to make certain subsequent matrix calculations simpler. However, it is more superior to analyze the linear data rather than the strongly non-linear EEG. Finally, as for RQA, it quantifies the number and the duration of the recurrences which presented by its phase space trajectory and has been widely used in the nonlinear data analysis. Nevertheless, it requires the computation cost of quantitative measures. Certainly, since each method has its property and limitation, the purposes of the characterizations are crucial for choosing the most appropriate one.

After EEG signals processing, several characteristics have been extracted and denoted as the features employed to study the behaviors of the brain and realize the objectives such as classification and detection. As found, the existing features contain a lot of statistical parameters such as mean, standard deviation, zero-crossing rate, root mean square (RMS), etc. [18]; the entropies like approximate entropy, sample entropy, phase entropy, and so on [19]; the chaotic parameters include largest Lyapunov exponent (LLE) and correlation dimension (CD) [20]; fractal dimension (FD) [21]; and brain rhythms [22]–[25] . Because the qualities of the features directly affect the performances of the EEG-based applications, thereby, an appropriate approach to extract and characterize the valuable features from the EEG signals is significant.

Among the above features, brain rhythms are one series of trustworthy patterns that have been commonly employed for EEG-based applications. Moreover, they are generated from the classifications of EEG signals based on the five specific sub-bands: delta (δ, 0–4 Hz), theta (θ, 4–8 Hz), alpha (α, 8–13 Hz), beta (β, 13–30 Hz), and gamma (γ, 30–50 Hz) [26]. In fact, the effect of the brain rhythms is that the presence or change of certain brain rhythms can be considered as clues to recognize and detect mental diseases, neurological disorders, and affective reactions [22]–[25]. For instance, the changes in α power can significantly indicate sleep disorders [22]. In Alzheimer's disease (AD), compared with the healthy subjects, the indications of amplitude increase in δ and θ sources, and the amplitude decrease in α and/or β sources can be detected in the patients [23]. As for affective reactions, the changes of power in γ are usually related to happiness and sadness [24], α power varied with the level of valence [25], and so on. Categorically, the brain rhythms are deliberated as the fundamental or key components in the frequency domain representations of EEG signals. However, the rhythmic time behaviors, i.e., the indications and consecutive existences of the brain rhythms, which are useful information to interpret the EEG with great details, have not been investigated yet. To study such chronological orders of the brain rhythms, the particular one which is appropriate to distinguish the specific brain state can be identified so that the details about the time-related transformations between different brain states can be determined. Meanwhile, the characteristics of the particular rhythm patterns are also useful for investigating the effect of subject-dependent in a specific brain state. On the other hand, based on the similarity measurement of the rhythm patterns among different channels, the signals synchrony in terms of rhythms synchronization can be indicated, which provides a solution to decrease the number of applied channels by mean of selecting several representatives. Thereby, to focus on the properties of the brain rhythms in their corresponding times of occurrences could extend the analysis and characterization of EEG signals in a new way. Then, inspired by the sequence analysis in bioinformatics, a technique named brain rhythm sequencing which interprets and characterizes the EEG as the sequence data consisted of the five specific brain rhythms has been proposed in this work. Moreover, this idea can be tested and employed for various EEG-based applications such as the detections of some neurological disorders.

Consequently, epileptic seizure detection, one of the conventional EEG-based detections, has been adopted as a case study to validate and evaluate the performance of the proposed brain rhythm sequencing technique.

The rest of this work is arranged as follows: Section II describes the details about the brain rhythm sequencing technique. Then, a case study of epileptic seizure detection is elaborated in Section III followed by the experimental results and discussion in Section IV. Finally, the conclusion of this work is provided in Section V.

II. METHODOLOGY

The proposed technique contains three main phases: A) sequence production by selecting the prominent brain rhythm at specific timestamp consecutively throughout the EEG; B) sequence analysis based on the selection of representatives to reduce the number of applied channels; and C) sequence characterization for the case study of seizure detection. First, since both the time and frequency information is significant for brain rhythm sequencing. Therefore, an appropriate TFA method has been applied. Afterward, in order to reduce the workload in handling multi-channel EEG data, the selection of the representative channels has been considered, i.e., the sequence analysis is for selecting the representatives and it is derived from rhythms synchronization through the similarity measurement of all generated sequences. Finally, sequence characterization is performed on those sequences from the representative channels and in order to realize the aim of seizure detection, two additional indices that reflect power discharge of the signals and synchronous behavior of the brain rhythms have been used. The following sub-sections describe the above phases in detail.

A. SEQUENCE PRODUCTION BY TFA

The brain rhythm sequencing is referring to a technique that interprets the EEG signals in chronological order by means of five brain rhythms. Certainly, its production needs specific brain rhythm (frequency information) at a certain timestamp (time information). In this regard, the instantaneous power distributions in the time-frequency plane can provide more details to characterize the EEG signals appropriately and hence, TFA, which decomposed the signals into the time-frequency domain simultaneously, has been considered. As for TFA, WVD is a typical method that has been applied to calculate the instantaneous time-frequency information and the power distributions of signals [16], which also belongs to standard Cohen's class in the time-frequency distributions. By employing WVD, the information about the instantaneous power in the time-frequency localizations of the signals can be acquired, which enables the application for evaluating the power value in specific sub-band of frequency and to localize it into the corresponding timestamp [27]. Such properties are beneficial to study the details of the five brain rhythm at each timestamp and accomplish the brain rhythm sequencing from the whole signals. Mathematically, WVD is given by (1):

$$W_x(t,\omega) = \int_{-\infty}^{+\infty} x(t+\frac{\tau}{2})x^*(t-\frac{\tau}{2})e^{-j\omega\tau}d\tau \tag{1}$$

where $x(t)$ is the signal, t and ω correspond to the time and frequency respectively, and $*$ indicates complex conjugate of $x(t)$. But, WVD could generate unnecessary cross-terms that confine to calculate the time-frequency information accurately. Thus, to remove cross-terms, a further operation such as an appropriately smoothing way of WVD along the time as well as frequency direction is recommended [27]. Considering a separable smoothing function shown in (2):

$$W_h(t,\omega) = g(t)H(-\omega) \tag{2}$$

where $H(\omega)$ is the Fourier transform of smoothing window $h(t)$ in the frequency domain, and $g(t)$ is the smoothing window in the time domain. Then, $h(t)$ removes cross-terms in the frequency domain, while $g(t)$ reduces cross-terms in the time domain simultaneously. Therefore, the independent control has been adopted in both the time and frequency domains. This modified WVD version is smoothed pseudo WVD (SPWVD), as expressed in (3) [28]:

$$SPW_x(t,\omega) = \int_{-\infty}^{+\infty} h(\tau)\int_{-\infty}^{+\infty} g(s-t)x(s+\frac{\tau}{2})x^*(s-\frac{\tau}{2})e^{-j\omega\tau}dsd\tau \tag{3}$$

In (3), the independency between $h(t)$ and $g(t)$ helps SPWVD more flexible to solve the cross-terms. Besides, in order to obtain the precise time indices of the higher power regions and improve the meaningfulness of required power values in the time-frequency plane, reassignment operation is needed [28]. The principle of reassignment is to relocate each value of SPWVD at any point (t, ω) to another point $(\hat{t}, \hat{\omega})$, which is the center of gravity of the signals power distribution around (t, ω). Consequently, a reassigned value of SPWVD at any point $(\hat{t}, \hat{\omega})$ becomes the sum of all values reassigned to that point, as presented in (4):

$$SPW_x^{(r)}(t',\omega';g,h) = \int_{-\infty}^{+\infty}\int_{-\infty}^{+\infty} SPW_x(t,\omega;g,h)\,\delta(t'-\hat{t}(x;t,\omega))\delta(\omega'-\hat{\omega}(x;t,\omega))dtd\omega \tag{4}$$

where

$$\hat{t}(x;t,\omega) = t - \frac{SPW_x(t,\omega;\tau_g,h)}{2\pi SPW_x(t,\omega;g,h)} \tag{5}$$

$$\hat{\omega}(x;t,\omega) = \omega + j\frac{SPW_x(t,\omega;g,D_h)}{2\pi SPW_x(t,\omega;g,h)} \tag{6}$$

with $\tau_g = tg(t)$ and $D_h(t) = dh(t)/dt$.

The reassigned SPWVD (RSPWVD) not only assists to remove the interferences of cross-terms in both the time and frequency domains but also makes the power distributions have the proper representations in five specific brain rhythms

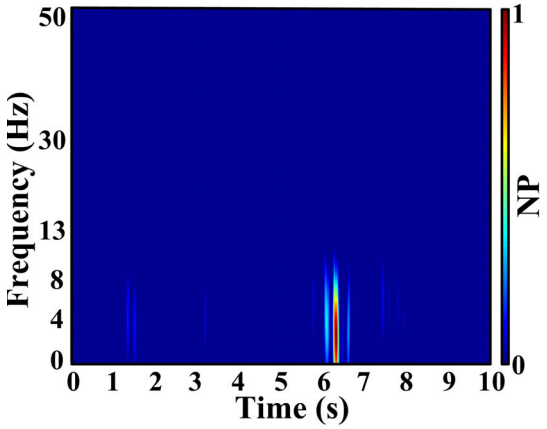

FIGURE 1. TFA of EEG from the C4 channel by using SPWVD followed by the reassignment operation. Label: NP means normalized power.

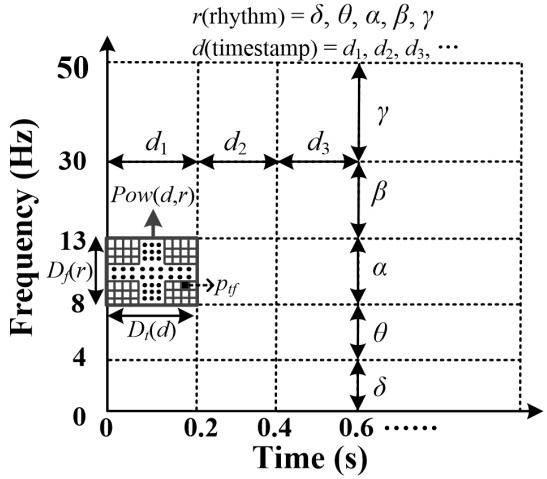

FIGURE 2. Power estimation of five brain rhythms at each timestamp by TFA (RSPWVD method); where *r* and *d* correspond to brain rhythm and timestamp respectively; *Pow(d,r)* presents the power value of one specific rhythm at a certain timestamp; p_{tf} indicates the instantaneous power in each bound of the time-frequency plane; $D_t(d)$ and $D_f(r)$ is the distance between adjacent timestamps and brain rhythms separately.

at each timestamp. Here, a TFA result of the EEG signals with 10 s length from the C4 channel has been depicted in Fig. 1, in which the horizontal and vertical directions denote the time in 0–10 s and the frequency in 0–50 Hz respectively, and the colors illustrate the normalized power (NP) ranged from 0 (deep blue) to 1 (deep red). The numbers along the vertical axis are the limiting values of five brain rhythms, i.e., the ranges of δ, θ, α, β, and γ.

To form the sequence, duration of timestamp (d) should be taken into account, i.e., the whole span of time of EEG is divided into d-segments for sequencing. On the other hand, the frequency is divided into five components based on brain rhythms (r). Therefore, in the time-frequency plane, there are five brain rhythms at each timestamp, as displayed in Fig. 2, in which the horizontal and vertical directions correspond to the time in s and the frequency in Hz. Indeed, the sequence data requires one element at each timestamp, not a group of them. Consequently, in order to choose the most significant

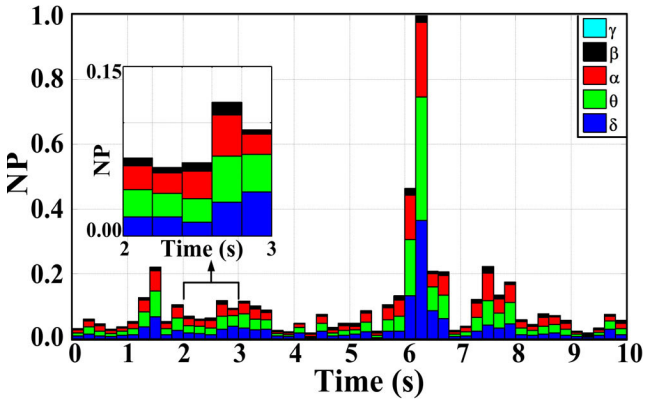

FIGURE 3. The cumulative NP values of the five brain rhythms at each timestamp of 0.2 s consecutively throughout the EEG signals.

one to represent each timestamp properly, the instantaneous power (p_{tf}) in each bound of the time-frequency plane has been considered. For instance, in Fig. 2, the $Pow\ (d, r)$ indicates the power value of one specific brain rhythm at a certain timestamp, which is calculated by the average of all the p_{tf} bounded in a range consisted by $D_t(d)$ and $D_f(r)$; where $D_t(d)$ corresponds to the duration of preset timestamp and $D_f(r)$ refers to the distance between adjacent brain rhythms separately. So, $Pow\ (d, r)$ denotes the effect of power contribution in the five brain rhythms (δ, θ, α, β, and γ) at each timestamp (d_1, d_2, d_3, …). Its calculation can be expressed as (7):

$$Pow(d, r) = \frac{\sum p_{tf}(D_t(d), D_f(r))}{D_t(d)D_f(r)} \tag{7}$$

Regarding $D_t(d)$, it decides the length of the brain rhythm sequence data and should be preset. As a measurement of potential variations induced by the firings of neurons, the responses of the brain have been recorded in the EEG and the analysis of EEG is the study of electrical activities of neurons. In this regard, to capture the responses of neurons is beneficial to analyze the EEG in detail and the average reaction time of neurons could imply a unit time period that the neurons are having reactions including the firings. In the previous EEG-based studies, Rey *et al.* [29] claimed that the average evoked power appears for a timestamp of 0.2 s by applying TFA. In [30], Chandra *et al.* mentioned that the average reaction time is 0.14–0.2 s. As found, 0.2 s can be regarded as a unit time period to capture the primary electrical responses of neurons and therefore, the timestamp of the brain rhythm sequence is set as 0.2 s. Then, at each timestamp of 0.2 s, there are five distinct power values located in various rhythms, as shown in Fig. 3, in which the horizontal and vertical directions refer to the timestamps (here, a 10 s EEG has been divided into 50 timestamps) and the cumulative NP values of the five rhythms respectively. Different colors mean the contributions of power through different rhythms. Besides, at each timestamp, considering the maximum one reflects the critical frequency component that has a relatively great contribution of power, it can be denoted as the most

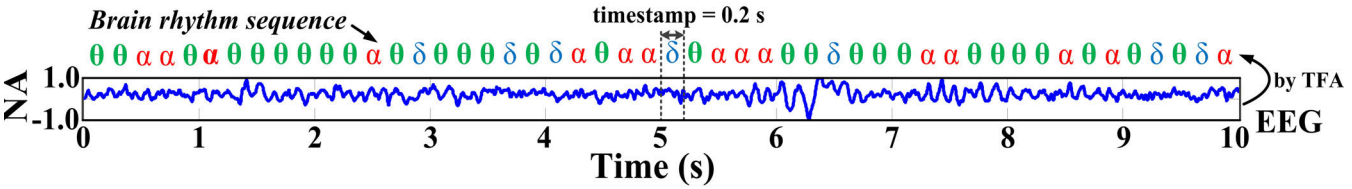

FIGURE 4. Brain rhythm sequencing from EEG signals based on choosing the prominent rhythm having the maximum power contribution at each timestamp of 0.2 s by TFA. Label: NA refers to normalized amplitude.

significant feature in the frequency domain for interpreting the EEG. Thus, via the calculations by TFA of EEG, the brain rhythm presents the maximum power contribution at each timestamp has been chosen for brain rhythm sequencing and Fig. 4 presents a sample of the generated brain rhythm sequence data from EEG, in which a 10 s EEG from the C4 channel lies at the bottom, and its corresponding rhythm patterns are displayed at the top.

B. SEQUENCE ANALYSIS BASED ON SIMILARITY

Because the brain rhythm sequence data is produced for the EEG signals on each scalp channel so that the number of the sequences equal to the number of channels in the EEG system, which could increase the workload to implement characterization in the next step. Hence, the reduction of the amount of channel by selecting representative sequences (channels) is desired. To this aim, considering the similarity analysis is generally applied for studying the properties of sequence data in bioinformatics and here, the similarity relationships of brain rhythm sequences can also imply the signals synchrony, along with indicating the connectivity between the EEG channels. Therefore, the selection of the representatives is by implementing the sequence analysis based on the rhythms synchronization among all pairs of generated sequences. Afterward, the selected sequences from the representative channels are employed for the characterizations of seizure detection. In this work, in order to indicate the synchronization level of the brain rhythms in the sequences, the similarity coefficient has been measured and it is evaluated by the Levenshtein distance, which is the minimum number of single-character edits (either insertions, deletions, or substitutions) required to change one code into the other [31]. If a system has 16 EEG channels, 16 brain rhythm sequences will be produced. Then, the Levenshtein distance between one pair of sequences a and b (from two different EEG channels) is given by (8):

$$lev_{a,b}(i,j) = \begin{cases} \max(i,j) & \text{if } \min(i,j)=0, \\ \min \begin{cases} lev_{a,b}(i-1,j)+1 \\ lev_{a,b}(i,j-1)+1 \\ lev_{a,b}(i-1,j-1)+indf_{(ai\neq bj)} \end{cases} & \text{otherwise.} \end{cases} \tag{8}$$

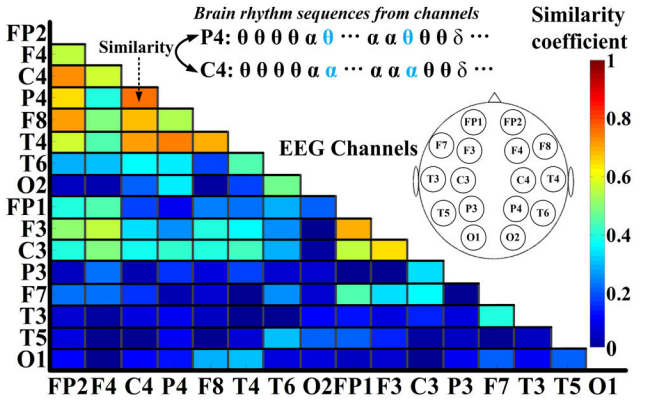

FIGURE 5. A sample result of the similarity coefficients derived from the Levenshtein distances among all pairs of generated brain rhythm sequences on corresponding EEG channels.

where

$$indf_{(ai\neq bj)} = \begin{cases} 0 & ai = bj, \\ 1 & \text{otherwise.} \end{cases} \tag{9}$$

In (8), $lev_{a,b}(i, j)$ means the distance between the first i pattern of sequence a and the first j pattern of sequence b. Then, the first element in the minimum of (8) corresponds to deletion (from a to b), the second to insertion, and the third to match or mismatch, depending on whether the respective rhythm patterns are the same. Meanwhile, *indf* in (9) is the indicator function and it equal to 0 when two sequences are the same. Certainly, the smaller the distance indicates the two sequences are more similar. Following the calculations based on the Levenshtein distance, the level of rhythms synchronization among all pairs of sequences can be identified and a sample result has been illustrated in Fig. 5, in which the horizontal and vertical directions show the 16 standard EEG channels: FP2, F4, C4, P4, F8, T4, T6, O2, FP1, F3, C3, P3, F7, T3, T5, and O1. The color reveals the level of the similarity coefficient (*simc*) from the normalized Levenshtein distance value that ranged into 0 (deep blue) to 1 (deep red) via (10), where 0 represents the least similarity and 1 refers to the strongest relationship.

$$simc = \frac{\max(lev_{a,b}) - lev_{a,b}}{\max(lev_{a,b})} \tag{10}$$

Next, the selection of the representatives is based on the summation by (11), where the rhythms synchronization (*ss*)

of one channel ch_a has been evaluated by considering the summation of all its *simc* values with other channels ch_o. Obviously, the higher *ss* can indicate this channel having stronger synchronous relationships with others. Hence, its rhythm pattern should appear frequently among all the sequences and could be regarded as representative. In this work, the channel having maximum *ss* and those if having *ss* values within 5% differences to the maximum ($\max(ss) \times 0.95$) are selected as the representatives. Thereby, based on the similarity study, the number of brain rhythm sequences for characterization can be significantly reduced.

$$ss(cha) = \sum_{cha \neq cho} simc(cha, cho) \tag{11}$$

C. SEQUENCE CHARACTERIZATION FOR DETECTION

Here, the sequence characterization has been performed on the representative channels selected from the above phase. Since seizure detection has been adopted as a case study for evaluation of the proposed technique, the main focus of the characterization is concentrated on detecting the abnormal seizures from the EEG signals and to this aim, several key points related to the seizure detection by using EEG signals have been considered.

Since epilepsy is characterized by recurrent seizures, which are transient and paroxysmal events produced by the abnormal electrical discharges and synchronous neuronal activities, thus, when seizures appear, the abnormalities in the electrical signals usually contain large power discharges and highly synchronous behaviors [32]. Seizure detection is a valuable tool for diagnosing epilepsy and the EEG-based seizure detection is a conventional manner as EEG records the electrical activities with good time resolution. Besides, TFA methods have been widely used for extracting suitable features in seizure detection. For instance, Zandi *et al.* [10] applied wavelet packet transform (WPT) in TFA for seizure detection and they developed the combined seizure index (CSI) calculated by the rhythmicity and relative energy of EEG. According to CSI, the alarm of seizure onset can be achieved. Further, the similar approaches by applying other TFA techniques can be found in [12], [16], [33], and so on.

Regarding the proposed technique, RSPWVD in TFA has been used to calculate instantaneous power in both the time and frequency domains. Therefore, the proposed technique is following a conventional manner to process the EEG signals. While the main difference is that the EEG signals have been represented by means of the chronological order based on the prominent rhythm having the maximum instantaneous power and expressed as brain rhythm sequence data. Then, via the sequence characterization, the time-related transformations between seizure/non-seizure intervals in the EEG could be distinguished by considering the presences or the changes of certain particular rhythm patterns so that the time-related occurrences of abnormal seizures can be determined properly. As found, when seizures appear, the abnormalities in EEG usually contain excessive electrical discharges and highly synchronous neuronal activities. So, to enrich the properties of the rhythm sequence for seizure detection, two additional indices that reflect power discharge (*pd*) and synchronous behavior (*sb*) have been developed.

TABLE 1. Indexing of synchronous behavior (*sb*) and power discharge (*pd*) for the proposed brain rhythm sequence data.

sb index		*pd* index		
Range of *syn*	*sb*	Pr£. of IRP§	Range of IRP	*pd*
0.0—0.09	0	90%≤Pr	IRP≤μ+1.05σ	0
0.1—0.19	1	80%≤Pr<90%	μ+1.05σ<IRP≤μ+1.11σ	1
0.2—0.29	2	70%≤Pr<80%	μ+1.11σ<IRP≤μ+1.19σ	2
0.3—0.39	3	60%≤Pr<70%	μ+1.19σ<IRP≤μ+1.29σ	3
0.4—0.49	4	50%≤Pr<60%	μ+1.29σ<IRP≤μ+1.41σ	4
0.5—0.59	5	40%≤Pr<50%	μ+1.41σ<IRP≤μ+1.58σ	5
0.6—0.69	6	30%≤Pr<40%	μ+1.58σ<IRP≤μ+1.82σ	6
0.7—0.79	7	20%≤Pr<30%	μ+1.82σ<IRP≤μ+2.23σ	7
0.8—0.89	8	10%≤Pr<20%	μ+2.23σ<IRP≤μ+3.16σ	8
0.9—1.00	9	Pr<10%	μ+3.16σ<IRP	9

Note: £ Probability; § Instantaneous Rhythm Power (IRP).

First, the *sb* index denotes the synchronous behavior of rhythm patterns among all generated sequences at the same timestamp. Definitely, the stronger synchronous behavior can be considered when a number of generated sequences reflect a consistent rhythm pattern at that timestamp. Here, the *sb* is evaluated based on *syn*(*d*,*r*), the ratio of rhythms synchronization, as expressed in (12):

$$syn(d, r) = \frac{N_s(d, r)}{N_{ch}} \tag{12}$$

where $N_s(d, r)$ means the number of sequences having the same type of rhythm pattern at the same timestamp, and N_{ch} is the total number of sequences. For instance, if the rhythm pattern of one sequence is θ at its first timestamp (d_1), then its *syn* of d_1 is the ratio of the number of sequences having θ in d_1 to the total number of sequences. As $0 \leq syn \leq 1$, the *syn* must be fractional. Thus, to make *sb* simpler and easily distinguished in the sequence, it has been defined by *syn* value following the left part of Table 1, in which the first two columns are the range of *syn* and the corresponding *sb* separately. Consequently, the higher *sb* implies the stronger synchronous behavior appeared at that timestamp, which reflected by consistent rhythm among all the sequences.

Second, the *pd* index has been adopted to indicate the strength of instantaneous rhythm power (IRP) at a certain timestamp. A sample result of the statistical distribution of IRP from one generated sequence (the sequence at the top of Fig. 4) has been illustrated in Fig. 6, in which the horizontal and vertical directions correspond to different IRPs based on the statistical intervals derived from the mean (μ) and standard deviation (σ), and the corresponding number

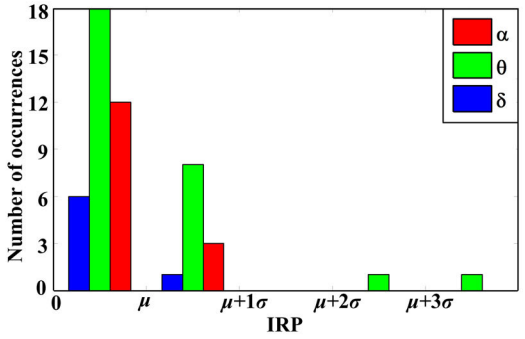

FIGURE 6. A sample result of statistical distribution of IRP from one generated rhythm sequence (the sequence at the top of Fig. 4).

Timestamp	d_1	d_2	...	d_{30}	d_{31}	d_{32}	d_{33}	d_{34}	...	d_{49}	d_{50}
F4 channel	θ_3^0	θ_6^0	...	α_6^0	θ_9^8	θ_9^9	δ_4^1	θ_8^0	...	θ_7^0	α_5^0
C4 channel	θ_3^0	θ_6^0	...	α_6^0	θ_9^8	θ_9^9	δ_4^1	θ_8^0	...	θ_7^0	α_5^0
P4 channel	θ_3^0	θ_6^0	...	α_6^0	θ_9^8	θ_9^9	θ_4^2	θ_8^0	...	θ_7^0	θ_4^0
T4 channel	θ_3^0	θ_6^0	...	α_6^0	θ_9^8	θ_9^9	θ_4^2	α_2^0	...	α_3^0	α_5^0
... channel			...						...		

FIGURE 7. Proposed brain rhythm sequence data with two additional indices (r_{pd}^{sb}) for representing the properties of EEG signals on different channels; where *pd* and *sb* are used for denoting the strength of power discharge of EEG and the level of rhythms synchronization respectively.

of occurrences respectively. As observed, the same rhythm has different IRP values. For example, for θ, most of them are located between 0 and $\mu+1\sigma$, while only two of them are beyond that interval. Therefore, based on such statistical intervals, the strength of IRP and the *pd* index can be estimated. In order to define these statistical intervals, Chebyshev's inequality presented in (13) has been applied. Then, according to (13), *pd* has been indexed based on the probability (*Pr*) at each decade, k (the distance of interval), μ, and σ, which summarized in the right part of Table 1. As a result, the high *pd* reveals the appearances of excessive power discharges at that timestamp.

$$Pr(|x-\mu| \geq k\sigma) \leq \frac{1}{k^2} \tag{13}$$

Finally, to comprise these two indices, the brain rhythm sequence can be expressed by r_{pd}^{sb} and Fig. 7 displays some samples on corresponding channels. In Fig. 7, it is clear that the timestamps of d_{31}–d_{32} present excessive discharges and highly synchronous behaviors simultaneously (empirically, both the indices *sb* and $pd \geq 8$), which implies the intervals of the abnormal seizures distinguishably. On the other hand, except for d_{31}–d_{32}, the indices of timestamps are relatively smaller, which also indicates that the duration of seizure or the time-related transformation between seizure/non-seizure intervals is about 0.4 s in Fig. 7. Moreover, concerning the corresponding rhythm pattern, θ has been identified, which indicates that θ should exhibit a certain relationship with seizure and hence, the change of θ is appropriate for seizure detection in this case. After the sequence characterization, the rhythmic characteristics of the EEG signals including the particular rhythm which is more significant for seizure detection and the time-related transformations between different states can be investigated. Next, an epileptic EEG database has been adopted as experimental verification for testing the proposed technique in a real application.

TABLE 2. The number of patients tested from Karunya database.

Group	Female	Male	Total
Child	10	7	17
Youth	8	10	18
Adult	8	9	17
Middle-age	11	13	24
Elderly	8	9	17
All	45	48	93

III. EXPERIMENTAL METHODOLOGY

A. DATABASE

Usually, data acquisition and pre-processing are the initial phases in EEG-based seizure detection. The raw signals are recorded by a number of electrodes placed on the scalp and after data recording, the pre-processing includes denoising by using conventional filtering and the artifacts removals have been operated. In this work, the data from an epileptic EEG database [34] provided by the Karunya University in India has been adopted for evaluating the performance of the proposed technique.

Karunya database contains a large number of patients with a very wide range of age and until now, the studies related to this database are limited, so it has been selected as the case study of seizure detection in the experimental verification. Moreover, the database comprises 174 patients (95 males and 79 females), and their ages vary from 1 to 84 years. Besides, the EEG system used is standard 10–20 and the number of channels is 18, in which 16 scalp channels and 2 periocular channels with the references to right and left mastoids. The sampling rate is 256 Hz and the analog passband of 0.01–100 Hz has been applied for the data pre-processing. For each patient, the time epoch of EEG data is 10 s and the events of abnormal seizures such as the spikes and sharp waves have been denoted. In this experiment, first, all the patients have been divided into five groups based on their ages: child (1–14 years), youth (15–28 years), adult (29–44 years), middle-age (45–65 years), and elderly (over 65 years). Afterward, 93 patients have been chosen randomly for investigations, i.e., 93 sets of EEG signals and each size is 16 scalp channels $\times$ 10 s. The details have been summarized in Table 2, in which the first column presents the group and the rest corresponds to the number of patients tested in this work.

B. EXPERIMENTAL DESIGN

The experiments based on seizure detection by applying the Karunya database have been designed into the following three main stages:

1) *Method validation*. The proposed technique has been validated based on its ability to detect abnormal seizures. In this regard, two conventional approaches, WT by Daubechies-4 (DB-4) wavelet [35] and ICA by InfoMax algorithm [36], have been employed for the same epileptic EEG from the database, along with using the proposed brain rhythm sequencing method. Afterward, the detections from three approaches are compared with the seizures related information from the database so that the capability of correct detection by applying the proposed method can be investigated.
2) *Seizure characterization*. The rhythmic characteristics of the epileptic EEG signals, especially the particular rhythm patterns related to the states of seizures, have been studied. Besides, the representative channels selected by the proposed rhythms synchronization principle have been inspected via a comparison with several conventional similarity measurements such as coherence, correlation, and mutual information.
3) *Performance evaluation*. The performance evaluation of the proposed technique has been accomplished based on a comparative study with several existing related works.

IV. RESULTS AND DISCUSSION

A. METHOD VALIDATION

In the method validation, two conventional methods, ICA, a statistical technique, and WT, a core TFA technique, have been implemented for comparisons. In this connection, the proposed method also combines both the statistical concept and TFA together. For instance, TFA helps to distinguish the prominent rhythm having the maximum instantaneous power at each timestamp of 0.2 s, and the statistical concept based on the Chebyshev's inequality assists to determine the statistical intervals that present excessive discharges of IRPs, i.e., to estimate the high *pd* index for the sequence data, which is one of the key factors for seizure detection.

Regarding ICA, it has been implemented by the InfoMax algorithm, which decomposes and makes the time course of electrical activities in one component spatially filtered from the channel data. On the other hand, since Liu *et al.* [35] claimed that the DB-4 wavelet has a similar shape and time-frequency characteristics with the seizures, which is more appropriate to detect the changes of epileptic EEG. Therefore, the DB-4 wavelet in WT can be considered as a technique to decompose the EEG signals into specific sub-bands for identifying abnormal seizures.

A result of detection by studying the EEG from epileptic patient A0043 in the database [34] has been depicted in Fig. 8. First, the epileptic EEG signals have been presented in Fig. 8(a), in which the names of 16 channels are shown along the vertical axis. The abnormalities of sharp waves (between 6 s and 7 s) have been highlighted by the deep red dots, i.e., the seizures happen at 6–7 s. Then, Fig. 8(b) is by ICA, in which the independent components from all

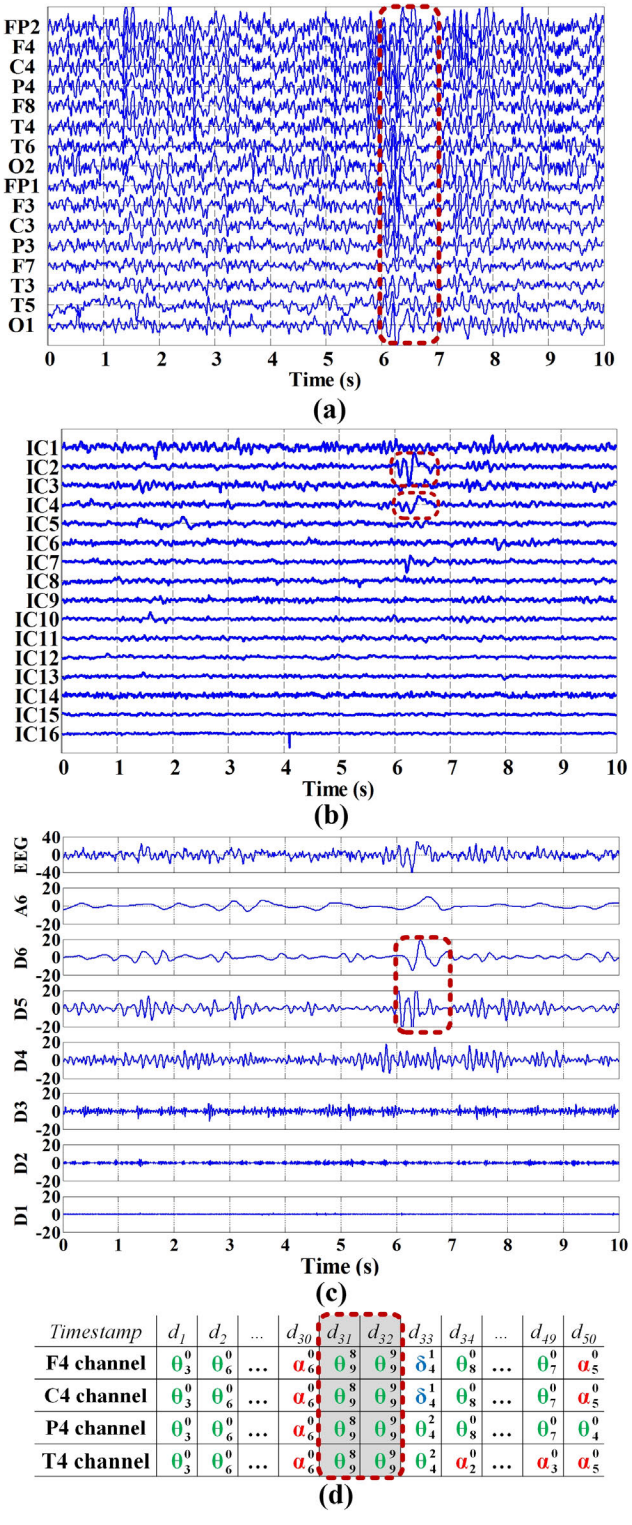

FIGURE 8. Seizure detection by conventional and proposed methods. (a) EEG signals with seizures; (b) and (c) are using conventional seizure detections by ICA and WT respectively; (d) is from the proposed brain rhythm sequencing. (Data is from Patient A0043 in Karunya database).

16 decompositions (IC1–IC16) have been depicted along the vertical axis. In ICA, any one of the ICs which present the larger amplitudes discharge (exceed about two-three times

compared with the background of amplitude) can be further considered as the abnormalities of EEG signals [36]. So, the intervals of seizures can be identified via the detections of such abnormalities and here, at 6–7 s, the larger amplitudes discharges can be found in IC2 and IC4 obviously, which implies the seizures should locate within 6–7 s. Next, the seizure detection by WT is in Fig. 8(c) and the decomposed signals (A6, D6, D5, D4, D3, D2, and D1) are illustrated along the vertical direction. In WT, since the majority of seizure activity is usually paroxysmal and the amplitude relative to the background would increase when seizures occur. Thereby, the large relative amplitude values usually accompany the seizures and the relative amplitude of each wavelet decomposition can be applied for detecting seizures properly [35]. Here, it can be found that the large relative amplitude values located within 6–7 s in both D6 and D5, which indicates the seizures existed in 6–7 s. Finally, the detection by the proposed method has been displayed in Fig. 8(d), in which the first row corresponds to the timestamps, and the rest presents the generated rhythm sequence data on the representative channels (F4, C4, P4, and T4). Based on the thresholds of two indices *sb* and *pd* (empirically ≥ 8), the intervals of abnormal seizures can be distinguished at the timestamps of d_{31}–d_{32}, i.e., about 6–6.4 s of the EEG. Meanwhile, those corresponding rhythm at the intervals of seizures is θ, indicating for the patient A0043, the particular rhythm pattern which is appropriate for seizure detection is θ. Besides, all of the detections are also consistent with the information provided in the database and thus, it can be said that the proposed brain rhythm sequencing is competent to detect abnormal seizures from the EEG signals.

B. SEIZURE CHARACTIERZATION

The seizure characterization is concerned with investigating the findings of representative channels and the results about the particular rhythm patterns identified from brain rhythm sequences on those representatives.

According to the summation of similarity coefficients by (11), the channels presenting higher values have been regarded as the representatives and characterized for seizure detection. Now, the significances of these channels have been inspected with the similarity measurements including coherence (frequency domain) which reveals how one EEG signals corresponds to others at each sub-band [37], and correlation (time domain), a measurement that determines whether and how pairs of EEG signals are related strongly [37]. Moreover, mutual information, which evaluates the inter-dependence between the signals using the concept of entropy in information theory, is also a typical method to investigate the similarity of EEG signals [38]. So, to inspect the representative channels, coherence, correlation, mutual information, and the proposed brain rhythm sequencing have been implemented for channel selection based on the similarity measurement simultaneously.

Here, all conventional methods have been performed on EEG signals from the database and then compared with the results from the proposed similarity study by using rhythm sequences. Such comparisons not only inspect whether the proposed brain rhythm sequence can interpret the rhythmic characteristics of EEG signals suitably but also identify if the selection of representative channels based on similarity analysis is reasonable or not. Further, (14), (15), and (16) have been adopted to calculate the value of coherence (C), correlation (r), and mutual information (I) between one pair of the EEG signals respectively: the coherence between two signals x and y at frequency f is by (14), where $G_{xy}(f)$ means the cross-spectral density between x and y at frequency f, and $G_{xx}(f)$ and $G_{yy}(f)$ are the auto spectral density of x and y at the frequency f respectively; the correlation between two signals x and y is from (15), where x and y are the two sets of signals, and i and j are those elements of each set. Then, the $\bar{x}$ and $\bar{y}$ refer to the means of x and y respectively; the mutual information between two signals x and y is based on (15), where $H(x)$ and $H(y)$ mean the marginal entropies of signals x and y respectively, and $H(x, y)$ represents the joint entropy of two signals x and y. After the above calculations, to select the representative channels based on the coherence, correlation, or mutual information, for each channel, all its values of C, r, or I with other channels have been summed separately. Then, in each measurement, the one having the maximum summation and those if having values within 5% differences to the maximum (max $\times$ 0.95) are selected as the representatives, which is the same principle adopted in the selection based on the proposed rhythm sequences.

$$C_{xy}(f) = \frac{\left|G_{xy}(f)\right|^2}{G_{xx}(f)G_{yy}(f)} \tag{14}$$

$$r_{xy} = \frac{\sum_i \sum_j (x_{ij} - \bar{x})(y_{ij} - \bar{y})}{\sqrt{(\sum_i \sum_j (x_{ij} - \bar{x})^2)(\sum_i \sum_j (y_{ij} - \bar{y})^2)}} \tag{15}$$

$$I(x; y) = H(x) + H(y) - H(x, y) \tag{16}$$

A set of the scalp maps (by EEG data of patient A0043 from [34]) consisted of 16 channels have been illustrated in Fig. 9 (scale in red color), in which the deeper the red represents the channel has a stronger synchronous behavior through the similarity measurements between itself and all the others. Consequently, those channels in the deep red can be selected as the representatives in terms of the signals synchrony. Moreover, Fig. 9(a), (b), (c), and (d) are the results by using coherence, correlation, mutual information, and the proposed brain rhythm sequencing respectively. In Fig. 9, it is clear that the representative channels found are mainly concentrated on the right hemisphere, especially in F4, C4, P4, and T4. Additionally, the statistical results of the representative channels from all 93 patients have been presented in Table 3, in which the first column refers to the 16 scalp channels, and the rest displays the proportions among 93 patients.

According to Table 3, it is found that the primary region of the representative channels is located in F4, C4, P4, and

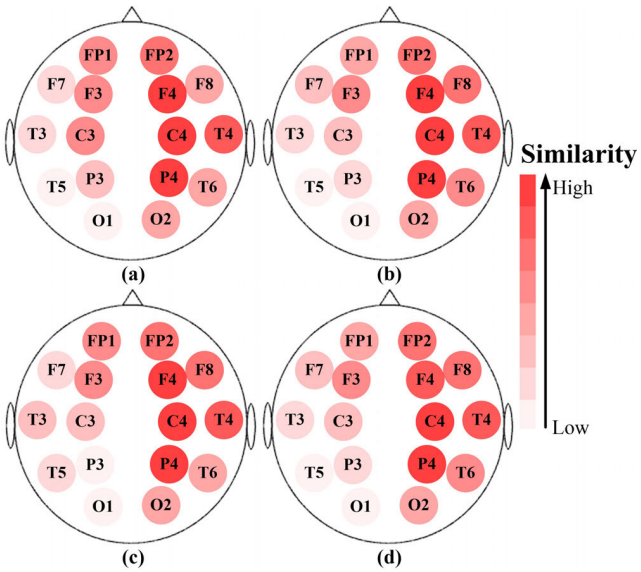

FIGURE 9. Scalp maps consisted of 16 channels based on similarity measurements by conventional and proposed methods. (a) Coherence; (b) Correlation; (c) Mutual information; (d) Brain rhythm sequencing. The deeper the red indicates it can be selected as the representative channels in terms of the signals synchrony. (Data is from Patient A0043 in Karunya database).

TABLE 3. Results of representative channels based on proportions.

Channel	Coherence	Correlation	Mutual information	Rhythm sequencing
FP2	23.66%	21.51%	31.18%	24.73%
F4	**84.95%**	**81.72%**	**82.80%**	**74.19%**
C4	**83.87%**	**80.65%**	**79.57%**	**73.12%**
P4	**60.22%**	**68.82%**	**63.44%**	**64.52%**
F8	6.45%	13.98%	10.75%	12.90%
T4	**66.67%**	**59.14%**	**52.69%**	**60.22%**
T6	7.53%	11.83%	5.38%	8.60%
O2	4.30%	11.83%	6.45%	4.30%
FP1	2.15%	5.38%	9.68%	10.75%
F3	5.38%	1.08%	3.23%	7.53%
C3	8.60%	9.68%	3.23%	11.83%
P3	6.45%	2.15%	7.53%	9.68%
F7	0.00%	1.08%	1.08%	0.00%
T3	3.23%	6.45%	4.30%	7.53%
T5	0.00%	1.08%	4.30%	1.08%
O1	2.15%	0.00%	3.23%	1.08%

T4 through both the conventional and proposed methods. Meanwhile, similar statistical results can also reveal that the proposed rhythm sequence data with the timestamp of 0.2 s is suitable for interpreting the rhythmic characteristics of EEG. Hence, by focusing on the rhythm sequences from the representatives, the properties of seizures can be studied by less number of applied channels.

Next, the particular rhythm pattern which is appropriate for seizure detection has been discussed. This part has been explained by considering another patient A0002 from [34]

TABLE 4. Particular brain rhythm detected by the proposed technique.

Database	No. of Patients	Brain rhythm					SD[£] (s)
		δ	θ	α	M[§]	U[†]	
Karunya [34]	93	15	47	26	4	1	0.2–1.0

Note: § Multiple types; † Undetected; £ Seizure duration.

Timestamp	...	d_{12}	d_{13}	d_{14}	d_{15}	d_{16}	d_{17}	...	d_{36}	d_{37}	d_{38}	d_{39}	...
F4 channel	...	θ_6^2	α_8^8	α_9^9	α_9^9	α_8^9	δ_6^0	...	θ_5^0	α_8^8	α_8^8	α_6^0	...
C4 channel	...	α_3^0	α_8^0	α_9^8	α_9^9	θ_2^3	δ_6^0	...	α_4^0	α_8^8	α_8^8	α_6^0	...
P4 channel	...	θ_6^0	α_8^0	α_9^8	α_9^8	θ_2^0	δ_6^0	...	θ_5^0	α_8^9	α_8^8	β_1^0	...
T4 channel	...	θ_6^0	α_8^0	α_9^3	α_9^8	α_8^9	θ_3^0	...	θ_5^0	α_8^8	α_8^8	α_6^2	...

FIGURE 10. Brain rhythm sequences on the representative channels (F4, C4, P4, and T4) for seizure characterizations, including the particular rhythm pattern appropriate for seizure detection and the time-related transformations between the seizure/non-seizure intervals. (Data is from Patient A0002 in Karunya database).

and the brain rhythm sequences on the representatives have been depicted in Fig. 10, in which the first row denotes the timestamp based on 0.2 s, and the rest shows the sequences with two additional indices. In Fig. 10, the representative channels present the high synchronizations and excessive discharges simultaneously (both the two indices $\geq$8) more than one time. For example, in F4, d_{13}–d_{16} and d_{37}–d_{38}; in C4 and P4, d_{14}–d_{15} and d_{37}–d_{38}; and in T4, d_{15}–d_{16} and d_{37}–d_{38}, which all depicted in gray color. Hence, these durations can be regarded as the intervals of seizures. In contrast, the non-seizure intervals are outside the mentioned intervals. As found, different channels have high indices at different timestamps, indicating their onsets and ends of seizures are not always the same. It is because the electrical discharges during seizures usually spread over a region, not at a point.

In addition, the instantaneous powers are very strong so that the excessive discharges can affect and spread to the nearby channels. Such results imply that abnormal seizures can be captured at certain timestamps on the specific channels by using the proposed technique. On the other hand, in the previous example (see Fig. 8(d)), θ rhythm appears during the seizure; whereas in Fig. 10, α rhythm occurs during the seizure. So, it indicates that the particular rhythm pattern related to seizure detection should be subject-dependent. Then, the statistical results of the particular rhythm pattern from all 93 patients have been summarized in Table 4 and the categories contain δ, θ, α, multiple types (like [δ, α], [δ, θ, α], etc.), and undetected. In Table 4, except the 4 successful detections with multiple types and the 1 failed detection, 15 have δ, 47 show θ, and 26 present α. As a result, it demonstrates that the particular brain rhythm related to the seizure should be δ, θ, and α. In the previous work [39], Saab *et al.* claimed that the efficient frequency band employed for seizure detection lies between 3–29 Hz, i.e., δ, θ, and α rhythms cover the entire range of such frequency band. Thus, the proposed method can distinguish the particular rhythm pattern during seizure specifically and by focusing on the changes of such rhythm through the two additional

TABLE 5. Comparative study of EEG-based seizure detection works.

	Database	No. of patients	Single/Multi-channel data	Channel selection	Methodology	Feature	Accuracy
Samiee *et al.* [33]	Bonn	10	Single	N/A	Rational discrete short-time Fourier transform	Power spectrum	98.1%
Wang *et al.* [40]	Own	10	Multiple	No	Partial directed coherence analysis	Inflow and outflow information	98.3%
Kumar *et al.* [41]	Bonn	10	Single	N/A	Artificial neural network	Entropies	94.5%
Martis *et al.* [42]	Bonn	10	Single	N/A	Empirical mode decomposition	Spectral peaks, spectral entropy, and spectral energy	95.3%
Yuan *et al.* [43]	Freiburg	21	Multiple	No	Extreme learning machine	Fractal geometry and relative fluctuation index	94.9%
Fan *et al.* [44]	CHB-MIT	23	Multiple	No	Complex recurrence network	Spectral graph theoretic features	98.5%
Aldana *et al.* [45]	Own	14	Multiple	No	Canonical polyadic decomposition and block term decomposition	Three-way tensor with frequency × time × channels	98.7%
Yuan *et al.* [46]	CHB-MIT	23	Multiple	Yes	Multi-view deep learning framework	Spectrogram fragments and channels information	94.0%
Wen *et al.* [47]	Bonn + CHB-MIT	10 + 23	Single + Multiple	N/A + Yes	Deep convolution network and autoencoders-based model	Unsupervised features via multiple convolution kernels in the network	94.3%
This work	**Karunya**	**93**	**Multiple**	**Yes**	**Reassigned SPWVD method**	**Brain rhythm sequence data**	**98.9%**

indices (*pd* and *sb*), the time-related occurrences of seizures can be determined reliably.

C. PERFORMANCE EVALUATION

In the performance evaluation, a comparative study has been conducted on the basis of detection accuracy (i.e., correct rate) with several existing EEG-based seizure detection works and the details have been summarized in Table 5, in which the first two columns show the works and their applied database, and the rest presents the number of patients tested, the type of EEG based on single-channel or multi-channel, the operation of channel selection, methodology, the related features, and the seizure detection accuracy correspondingly.

Previously, as the rhythmic time behaviors have not been considered yet. Hence, the brain rhythm sequencing has been proposed to fill this gap. Further, via the proposed technique, the particular brain rhythm which is appropriate to detect the abnormal seizures can be determined and by focusing on its changes, the transformations between the seizure/non-seizure intervals can be identified in detail. Such findings not only offer insights into the epileptic EEG signals in terms of brain rhythm activities but also provide a novel way to investigate the effect of subject-dependent in the seizure. Besides, in the previous works, the studies by using the Karunya database are limited and it has not been chosen as the testing database yet. So, it is applied for experimental verification in this work and the successful detections for 92 of 93 patients (98.9%) can be accomplished, which demonstrates that the proposed technique is reliable for the patients with various ages (from 1 to 84 years) and further, their rhythmic characteristics can also be extracted for achieving EEG-based seizure detections.

On the other hand, regarding the types of EEG data, for the studies by single-channel, it is not necessary for them to select the representative channels because they have not considered the spaces or locations information. Nonetheless, for the multi-channel, the channel selection not only reduced the workload of further analysis but also helps to decrease the dimensionality so that fewer sensors are required in the real equipment. As seen, most of the previous works ignored such selection issues and only focus on detection via developing special features or classifiers. Additionally, although several works [46], [47] have performed the selection, they have not provided the details or results about the selected channels and meanwhile, the statistical analysis among different patients was also missing. Hence, by mean of the similarity analysis of the brain rhythm patterns in the proposed sequences, the synchrony of signals has been evaluated and such operation is helpful for selecting the representatives of each patient. Besides, based on the representatives from different patients, a statistical result among 93 patients has also been realized, where F4, C4, P4, and T4 have been found.

Currently, the deep learning-based methods are popular for EEG-based seizure detection [46], [47]. In deep learning, the applied multi-layer neural networks are able to learn the high-level or most relevant features from the input EEG data in an incremental manner. Consequently, the advantage of the deep learning-based method is that it can eliminate the requirement for significant feature extraction and is superior to acquire the unsupervised features from the unlabeled EEG.

Certainly, using the neural networks, abnormal seizures can be detected automatically from the unlabeled EEG with high accuracy. But in deep learning, the locations of representative channels and the particular rhythm patterns related to the seizure, which are valuable information to study individual characteristics of EEG, are not included. So, the brain rhythm sequencing has been proposed to investigate those rhythmic characteristics and perform the channel selection for seizure detection, which has not been discussed in the previous deep learning-based methods. Besides, deep learning is proper for the larger data size such as the long hours

EEG recordings, because the high-dimension data is more superior for training the neural networks model. However, when the data size is smaller, deep learning may meet the challenge to train the model. In this regard, the proposed technique is suitable to process the small data size since the EEG signals have been characterized into brain rhythm sequence data rather than the traditional training and testing for establishing a classification model. Hence, different approaches can be applied to analyze different data sizes in EEG-based seizure detection.

V. CONCLUSION

To verify the proposed brain rhythm sequencing technique and evaluate its performance in the EEG signals analysis, a case study of seizure detection for 93 patients from the Karunya database has been implemented. Results show that the particular rhythm pattern related to abnormal seizure is subject-dependent and for almost all cases, it is either δ, θ, or α. Thus, by focusing on the changes of particular rhythm via two additional indices, the time-related transformations between seizure/non-seizure intervals can be determined. Besides, the representative channels for seizure detection can be selected based on rhythms synchronization, which also helps to reduce the number of applied channels. Finally, since the detection accuracy has been accomplished up to 98.9%, it can be said that the proposed technique is appropriate for characterizing EEG and performing seizure detections for epileptic patients.

On the other hand, the RSPWVD method in TFA has been adopted in the initial step and since its calculation is relatively time-consuming, the sequencing for long hours EEG signals will be challenging. Besides, by developing specific characterizations or extracting significant rhythmic features from the generated sequences, other EEG-based applications such as emotion recognition and the fatigue or mental monitoring will also be studied in the future works.

REFERENCES

[1] A. Ridouh, D. Boutana, and S. Bourennane, "EEG signals classification based on time frequency analysis," *J. Circuits, Syst. Comput.*, vol. 26, no. 12, 2017, Art. no. 1750198.

[2] S. Altunay, Z. Telatar, and O. Erogul, "Epileptic EEG detection using the linear prediction error energy," *Expert Syst. Appl.*, vol. 37, no. 8, pp. 5661–5665, 2010.

[3] L. Jäncke and N. Alahmadi, "Resting state EEG in children with learning disabilities: An independent component analysis approach," *Clin. EEG Neurosci.*, vol. 47, no. 1, pp. 24–36, 2016.

[4] G. D. Jacobs and R. Friedman, "EEG spectral analysis of relaxation techniques," *Appl. Psychophysiol. Biofeedback*, vol. 29, no. 4, pp. 245–254, 2004.

[5] D. J. Buysse, A. Germain, M. L. Hall, D. E. Moul, E. A. Nofzinger, A. Begley, C. L. Ehlers, W. Thompson, and D. J. Kupfer, "EEG spectral analysis in primary insomnia: NREM period effects and sex differences," *Sleep*, vol. 31, no. 12, pp. 1673–1682, 2008.

[6] A. T. Tzallas, M. G. Tsipouras, and D. I. Fotiadis, "Epileptic seizure detection in EEGs using time-frequency analysis," *IEEE Trans. Inf. Technol. Biomed.*, vol. 13, no. 5, pp. 703–710, Sep. 2009.

[7] R. J. Oweis and E. W. Abdulhay, "Seizure classification in EEG signals utilizing Hilbert-Huang transform," *Biomed. Eng. Online*, vol. 10, May 2011, Art. no. 38.

[8] V. Bajaj and R. B. Pachori, "Automatic classification of sleep stages based on the time-frequency image of EEG signals," *Comput. Methods Programs Biomed.*, vol. 112, no. 3, pp. 320–328, 2013.

[9] M. Qaraqe, M. Ismail, E. Serpedin, and H. Zulfi, "Epileptic seizure onset detection based on EEG and ECG data fusion," *Epilepsy Behav.*, vol. 58, pp. 48–60, May 2016.

[10] A. S. Zandi, M. Javidan, G. A. Dumont, and R. Tafreshi, "Automated real-time epileptic seizure detection in scalp EEG recordings using an algorithm based on wavelet packet transform," *IEEE Trans. Biomed. Eng.*, vol. 57, no. 7, pp. 1639–1651, Jul. 2010.

[11] M. Wu, T. Wan, X. Wan, Y. Du, and J. She, "Fast, accurate localization of epileptic seizure onset zones based on detection of high-frequency oscillations using improved wavelet transform and matching pursuit methods," *Neural Comput.*, vol. 29, no. 1, pp. 194–219, 2017.

[12] A. Bhattacharyya and R. B. Pachori, "A multivariate approach for patient-specific EEG seizure detection using empirical wavelet transform," *IEEE Trans. Biomed. Eng.*, vol. 64, no. 9, pp. 2003–2015, Sep. 2017.

[13] S. Santaniello, S. P. Burns, A. J. Golby, J. M. Singer, W. S. Anderson, and S. V. Sarma, "Quickest detection of drug-resistant seizures: An optimal control approach," *Epilepsy Behav.*, vol. 22, pp. S49–S60, Dec. 2011.

[14] M. Niknazar, S. R. Mousavi, B. V. Vahdat, and M. Sayyah, "A new framework based on recurrence quantification analysis for epileptic seizure detection," *IEEE J. Biomed. Health Inform.*, vol. 17, no. 3, pp. 572–578, May 2013.

[15] F. C. A. Fernandes, R. L. C. V. Spaendonck, and C. S. Burrus, "A new framework for complex wavelet transforms," *IEEE Trans. Signal Process.*, vol. 51, no. 7, pp. 1825–1837, Jul. 2003.

[16] A. T. Tzallas, M. G. Tsipouras, and D. I. Fotiadis, "Automatic seizure detection based on time-frequency analysis and artificial neural networks," *Comput. Intell. Neurosci.*, vol. 2007, Oct. 2007, Art. no. 80510.

[17] C. Lv, J. Zhao, C. Wu, T. Guo, and H. Chen, "Optimization of the end effect of Hilbert-Huang transform (HHT)," *Chin. J. Mech. Eng.*, vol. 30, no. 3, pp. 732–745, 2017.

[18] A. Dalton, S. Patel, A. R. Chowdhury, M. Welsh, T. Pang, S. Schachter, G. OLaighin, and P. Bonato, "Development of a body sensor network to detect motor patterns of epileptic seizures," *IEEE Trans. Biomed. Eng.*, vol. 59, no. 11, pp. 3204–3211, Nov. 2012.

[19] U. R. Acharya, F. Molinari, S. V. Sree, S. Chattopadhyay, K.-H. Ng, and J. S. Suri, "Automated diagnosis of epileptic EEG using entropies," *Biomed. Signal Process.*, vol. 7, no. 4, pp. 401–408, Jul. 2012.

[20] S. M. S. Alam and M. I. H. Bhuiyan, "Detection of seizure and epilepsy using higher order statistics in the EMD domain," *IEEE J. Biomed. Health Inform.*, vol. 17, no. 2, pp. 312–318, Mar. 2013.

[21] F. Zappasodi, E. Olejarczyk, L. Marzetti, G. Assenza, V. Pizzella, and F. Tecchio, "Fractal dimension of EEG activity senses neuronal impairment in acute stroke," *PLoS ONE*, vol. 9, no. 6, Jun. 2014, Art. no. e100199.

[22] S. C. Kim, M. H. Lee, C. Jang, J. W. Kwon, and J. W. Park, "The effect of alpha rhythm sleep on EEG activity and individuals' attention," *J. Phys. Therapy Sci.*, vol. 25, no. 12, pp. 1515–1518, Dec. 2013.

[23] R. Lizio, F. Vecchio, G. B. Frisoni, R. Ferri, G. Rodriguez, and C. Babiloni, "Electroencephalographic rhythms in Alzheimer's disease," *Int. J. Alzheimer's Disease*, vol. 2011, Mar. 2011, Art. no. 927573.

[24] S. Koelstra, C. Mühl, M. Soleymani, J. S. Lee, A. Yazdani, T. Ebrahimi, T. Pun, A. Nijholt, and I. Patras, "DEAP: A database for emotion analysis; using physiological signals," *IEEE Trans. Affect. Comput.*, vol. 3, no. 1, pp. 18–31, Jan./Mar. 2012.

[25] M.-K. Kim, M. Kim, E. Oh, and S.-P. Kim, "A review on the computational methods for emotional state estimation from the human EEG," *Comput. Math. Methods Med.*, vol. 2013, Feb. 2013, Art. no. 573734.

[26] S.-J. Choi and B.-G. Kang, "Prototype design and implementation of an automatic control system based on a BCI," *Wireless Pers. Commun.*, vol. 79, no. 4, pp. 2551–2563, 2014.

[27] M. Szmajda, K. Górecki, and J. Mroczka, "Gabor transform, SPWVD, Gabor-Wigner transform and wavelet transform—Tools for power quality monitoring," *Metrol. Meas. Syst.*, vol. 17, no. 3, pp. 383–396, 2010.

[28] S. Barma, B.-W. Chen, K. L. Man, and J.-F. Wang, "Quantitative measurement of split of the second heart sound (S2)," *IEEE/ACM Trans. Comput. Biol. Bioinf.*, vol. 12, no. 4, pp. 851–860, Jul./Aug. 2015.

[29] H. G. Rey, I. Fried, and R. Q. Quiroga, "Timing of single-neuron and local field potential responses in the human medial temporal lobe," *Current Biol.*, vol. 24, no. 3, pp. 299–304, Feb. 2014.

[30] A. M. Chandra, S. Ghosh, S. Barman, R. Iqbal, and N. Sadhu, "Effect of exercise and heat-load on simple reaction time of University Students," *Int. J. Occupational Saf. Ergonom.*, vol. 16, no. 4, pp. 497–505, 2010.
[31] B. Cao, Y. Li, and J. Yin, "Measuring similarity between graphs based on the Levenshtein distance," *Appl. Math. Inf. Sci.*, vol. 7, no. 1L, pp. 169–175, 2013.
[32] R. S. Fisher, W. E. Boas, W. Blume, C. Elger, P. Genton, P. Lee, and J. Engel, Jr., "Epileptic seizures and epilepsy: Definitions proposed by the international league against epilepsy (ILAE) and the international bureau for epilepsy (IBE)," *Epilepsia*, vol. 46, no. 4, pp. 470–472, 2005.
[33] K. Samiee, P. Kovács, and M. Gabbouj, "Epileptic seizure classification of eeg time-series using rational discrete short-time Fourier transform," *IEEE Trans. Biomed. Eng.*, vol. 62, no. 2, pp. 541–552, Feb. 2015.
[34] T. G. Selvaraj, B. Ramasamy, S. J. Jeyaraj, and E. S. Suviseshamuthu, "EEG database of seizure disorders for experts and application developers," *Clin. EEG Neurosci.*, vol. 45, no. 4, pp. 304–309, 2014.
[35] Y. Liu, W. Zhou, Q. Yuan, and S. Chen, "Automatic seizure detection using wavelet transform and SVM in long-term intracranial EEG," *IEEE Trans. Neural Syst. Rehabil. Eng.*, vol. 20, no. 6, pp. 749–755, Nov. 2012.
[36] S. Shimamoto, Z. J. Waldman, I. Orosz, I. Song, A. Bragin, I. Fried, J. Engel, Jr., R. Staba, A. Sharan, C. Wu, M. R. Sperling, and S. A. Weiss, "Utilization of independent component analysis for accurate pathological ripple detection in intracranial EEG recordings recorded extra- and intra-operatively," *Clin. Neurophysiol.*, vol. 129, no. 1, pp. 296–307, 2018.
[37] T. N. Alotaiby, S. A. Alshebeili, T. Alshawi, I. Ahmad, and F. E. A. El-Samie, "EEG seizure detection and prediction algorithms: A survey," *EURASIP J. Adv. Signal Process.*, vol. 2014, p. 183, Dec. 2014.
[38] W. T. Kerr, A. Anderson, H. Xia, E. S. Braun, E. P. Lau, A. Y. Cho, and M. S. Cohen, "Parameter selection in mutual information-based feature selection in automated diagnosis of multiple epilepsies using scalp EEG," in *Proc. 2nd Int. Workshop Pattern Recog. NeuroImag.*, Jul. 2012, pp. 45–48.
[39] M. E. Saab and J. Gotman, "A system to detect the onset of epileptic seizures in scalp EEG," *Clin. Neurophysiol.*, vol. 116, no. 2, pp. 427–442, 2005.
[40] G. Wang, Z. Sun, R. Tao, K. Li, G. Bao, and X. Yan, "Epileptic seizure detection based on partial directed coherence analysis," *IEEE J. Biomed. Health Inform.*, vol. 20, no. 3, pp. 873–879, May 2016.
[41] S. P. Kumar, N. Sriraam, P. G. Benakop, and B. C. Jinaga, "Entropies based detection of epileptic seizures with artificial neural network classifiers," *Expert Syst. Appl.*, vol. 37, no. 4, pp. 3284–3291, 2010.
[42] R. J. Martis, U. R. Acharya, J. H. Tan, A. Petznick, R. Yanti, C. K. Chua, E. Y. K. Ng, and L. Tong, "Application of empirical mode decomposition (EMD) for automated detection of epilepsy using EEG signals," *Int. J. Neural Syst.*, vol. 22, no. 6, 2012, Art. no. 1250027.
[43] Q. Yuan, W. Zhou, Y. Liu, and J. Wang, "Epileptic seizure detection with linear and nonlinear features," *Epilepsy Behav.*, vol. 24, no. 4, pp. 415–421, 2012.
[44] M. Fan and C.-A. Chou, "Detecting abnormal pattern of epileptic seizures via temporal synchronization of EEG signals," *IEEE Trans. Biomed. Eng.*, vol. 66, no. 3, pp. 601–608, Mar. 2019.
[45] Y. R. Aldana, B. Hunyadi, E. J. M. Reyes, V. R. Rodríguez, and S. Van Huffel, "Nonconvulsive epileptic seizure detection in scalp EEG using multiway data analysis," *IEEE J. Biomed. Health Inform.*, vol. 23, no. 2, pp. 660–671, Mar. 2019.
[46] Y. Yuan, G. Xun, K. Jia, and A. Zhang, "A multi-view deep learning framework for EEG seizure detection," *IEEE J. Biomed. Health Inform.*, vol. 23, no. 1, pp. 83–94, Sep. 2019.
[47] T. Wen and Z. Zhang, "Deep convolution neural network and autoencoders-based unsupervised feature learning of EEG signals," *IEEE Access*, vol. 6, pp. 25399–25410, 2018.

JIA WEN LI (S'13) received the master's degree in electrical and electronics engineering from the University of Macau, Macau, China, in 2015, where he is currently pursuing the Ph.D. degree in electrical and computer engineering. His current research interests include biomedical signals processing, affective computing, and human body communication.

SHOVAN BARMA (M'15) received the master's degree in very large scale integration (VLSI) design from Bengal Engineering and Science University, Howrah, India, in 2008, and the Ph.D. degree in electrical engineering from National Cheng Kung University, Tainan, Taiwan, in 2015. He is currently an Assistant Professor with the Indian Institute of Information Technology Guwahati, Guwahati, India. His current research interests include biomedical signals processing, affective computing, and VLSI design.

PENG UN MAK (S'88–M'97–SM'11) received the B.Sc. degree in electrical engineering from National Taiwan University, Taipei, Taiwan, and the M.Sc. and Ph.D. degrees in electrical engineering from Michigan State University, East Lansing, MI, USA. He was a Visiting Fellow with the Clare Hall, University of Cambridge, Cambridge, U.K., in 2018. Since 1997, he has been an Assistant Professor with the Department of Electrical and Computer Engineering, University of Macau, Macau, China. His current research interests include biosignal extraction and processing, bioelectromagnetism, human body communication, and body sensor networks. He is a currently a Life Member of the Phi Kappa Phi and an Invited Member of the Eta Kappa Nu (currently IEEE-HKN)).

SIO HANG PUN (S'11–A'12–M'12–SM'18) received the master's degree from the University of Porto, Porto, Portugal, in 1999, and the Ph.D. degree in electrical and electronics engineering from the University of Macau, Macau, China, in 2012. He is currently an Associate Professor with the State Key Laboratory of Analog and Mixed-Signal VLSI, University of Macau. His current research interests include biomedical electronic circuits, miniaturized sensors for biomedical applications, and human body communication.

MANG I VAI (M'92–SM'06) received the Ph.D. degree in electrical and electronics engineering from the University of Macau, Macau, China, in 2002. He has been involved in research in the areas of digital signals processing and embedded systems, since 1984. He is currently the Coordinator of the State Key Laboratory of Analog and Mixed-Signal VLSI and an Associate Professor with the Department of Electrical and Computer Engineering, University of Macau.